Cern chopper final report

F. Caspers, T. Kroyer, M. Paoluzzi
CERN, Geneva, Switzerland

Abstract

In the framework of HIPPI and the CERN Superconducting Proton Linac studies, the design for a beam chopper has been carried out. It is an integral part of the medium energy line and has to establish the required time structure of the beam by cutting out selected bunches from the continuous bunch train coming out of the 3 MeV RFQ. Due to the bunch spacing of 2.84 ns a system rise and fall time of 2 ns is required. The design, prototyping and testing of the slow wave structure used as kicker as well as that of the pulse generators required to drive it are reported.

1. INTRODUCTION

The beam chopper foreseen for the CERN Superconducting H^- Linac (SPL) has to establish the beam time-structure required by the downstream machines. This is achieved by deflecting towards the beam dump part of the continuous bunch stream exiting the 3 MeV radio frequency quadrupole (RFQ). This proton energy has been chosen as a compromise between beam dynamics considerations and the chopper amplifier. At lower energies a large emittance growth would result from the relatively long drift space housing the chopper, while a higher energy would make the amplifier requirements more demanding. In order to reduce the drive voltage the lattice was optimized such that the kick is amplified by a downstream quadrupole[i].

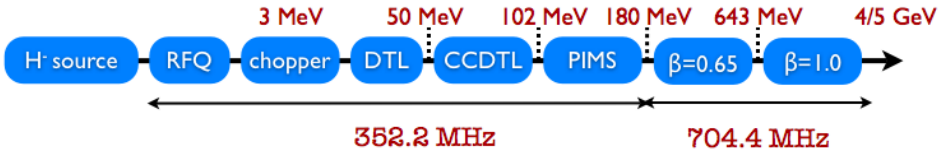

Figure 1: Schematic layout of the SPL

The chopper deflector comes in two identical units in series, each in a 50 cm long tank where 40 cm long deflecting plates are installed. To limit the chopper line length, the deflectors are installed inside two existing quadrupoles. Due to the slow beam velocity and the bunch spacing of 2.84 ns, up to six bunches will be on the chopper plates at the same time. To avoid partially chopped bunches, the rise time should be below 2 ns and the chopper kicker must operate as a travelling-wave structure matched to the speed of the beam (β=8%).

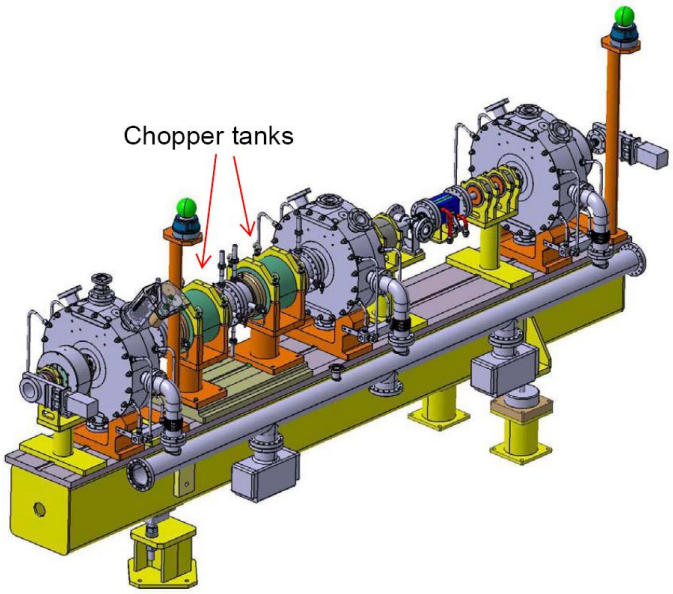

Figure 2: Integration of the chopper line.

The most stringent demand on the chopper comes from the operation for a Neutrino Factory, when it needs to remove three bunches out of eight in up to 0.6 ms bursts with a repetition rate of 50 Hz. This means driving the kicker with 44 MHz, 8.52 ns square pulses. Nevertheless, operation must be possible below 1 MHz, with 1 µs pulse lengths and 1 ms bursts. The plates are going to be driven at opposite polarities and the value of the effective voltage on each plate will be 400 V. Due to the fact the real structure has always less kick field than an ideal device with two infinitely extended planes (coverage factor < 1), voltages of the order of 600 V will have to be applied.

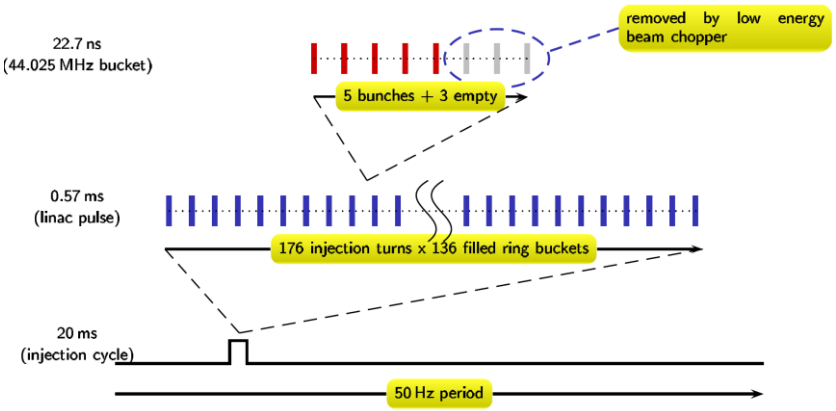

Figure 3: The timing scheme for "neutrino operation" (courtesy: F. Gerigk).

The distance between the two plates is 20 mm, which gives at total effective voltage of 800 V, a kick field of 40 kV/m and a deflection of 5.3 mrad. A beam dynamics simulation of the chopper line is shown in Fig. 4.

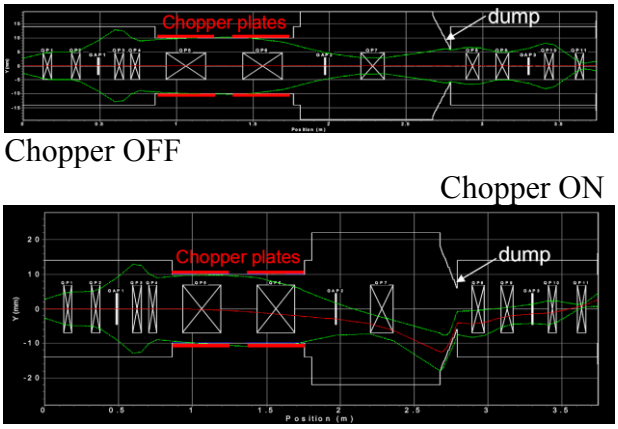

Figure 4: Beam dynamics simulation of the chopper line. (Courtesy: E. Sargsyan)

2. THE CHOPPER DEFLECTOR

The chopper has to fulfill tough electrical specifications, in particular the short rise time, low attenuation and the highest possible coverage factor. Errors in the line's electrical length cause the pulse to propagate at a different speed from the beam, thus possibly affecting adjacent un-chopped bunches. In addition it has to stand a significant amount of radiation and therefore a considerable heat load. It must operate in ultra-high vacuum and have sufficient high-voltage capabilities. Due to the given space constraints, a meander line structure appeared to be the most promising candidate for the design[ii]. When printed on a high permittivity substrate it is possible to reduce the transverse meander dimension and fit the chopper plates into the existing quadrupoles. Alumina (Al_2O_3, $\varepsilon_r \approx 9.8$) was chosen for the support because of its good radiation resistance (in particular compared to organic materials), good vacuum properties, good heat resistance and conduction and finally because a high ε implies small transverse meander size. For sufficient mechanical robustness, the substrate thickness of 3 mm was chosen. At first the parameters of a 50 Ω meander line were determined. However it turned out that the line width needs to be very close to the substrate height. In this case the spacing between parallel lines would be small, leading to high

dispersion. These problems could be avoided by combining two 100 Ω lines to form one 50 Ω double meander (Fig. 5).

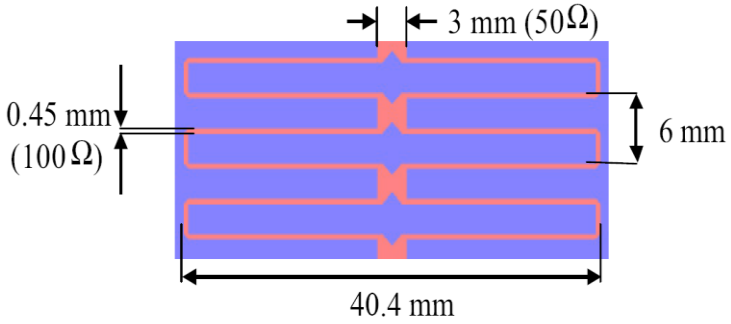

Figure 5: Geometry of the double meander line (version 2002).

First prototypes were manufactured at CERN but the final ceramic plates were produced in the industry by Kyocera. The manufacturing process went through many revisions and was adapted to the available technology. Fig. 6 shows the three layer final structure. First a 10 to 15 μm silver thick-film layer is applied on the ceramic plates. Then a 30 μm copper main conduction layer can be deposited electrochemically and finally a thin finishing of gold is applied for low contact resistance and as a protection against oxidation.

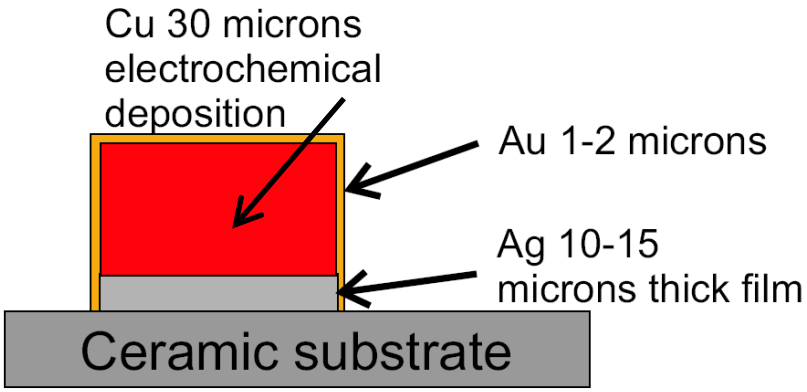

Figure 6: Kyocera plates layer structure.

In order to provide good mechanical stability for the ceramic plate a 10 mm thick, 70 mm wide and 46 cm long stainless steel plate is used as ground plane. The RF connections to the meander line are done with feed-throughs. Fine adjustment of the electrical length is foreseen by cutting longitudinal grooves under the ceramic plates. On the back of the ground plane the water cooling is installed. A small copper "scraper" is placed on the front side. It protrudes by ≈ 0.3 mm farther than the ceramic plate into the beam aperture to limit beam losses there. This should be effective in particular for the second chopper tank where the beam envelope has its maximum size (Fig. 4). For the first tank and for chopped beam, however, the scraper is not expected to reduce much the losses on the ceramic plates. Fig. 7 shows the chopper plates with the accessories. The ground plates are held in place by two support rings at the ends of the tank. Each of these rings can be aligned with three screws. This way the position of the plates can be easily adjusted. It is also possible to tilt them to change the kick strength or to reduce beam losses on the ceramic plates. The tank after installation of the first plate is shown in Fig. 8.

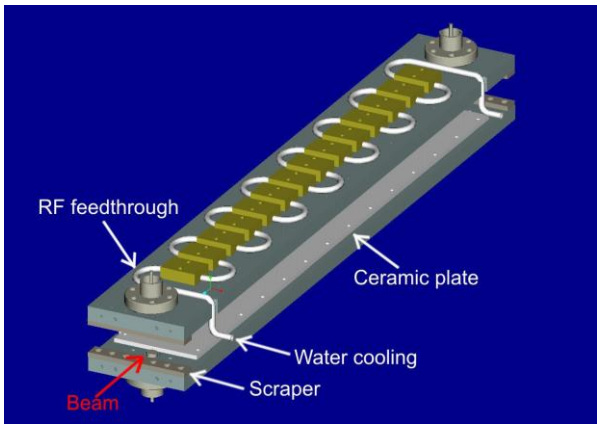

Figure 7: Two ceramic plates fixed on their support plates with the water cooling lines mounted on the back.

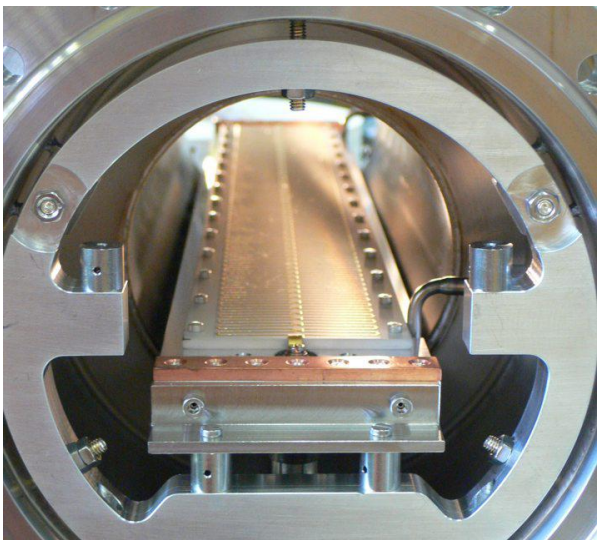

Figure 8: The first plate installed in the chopper tank.

A series of RF measurements were performed on the chopper plate. The transmission magnitude S_{21} of the single chopper plate is shown in Fig. 9. This attenuation was measured at the end of the plate. When averaged over the operational frequency range (≈200 MHz) and the plate length, it corresponds to 0.3 dB effective attenuation and to a kick field decrease of 3.4 %. At DC a resistance of 1.1 Ω was measured.

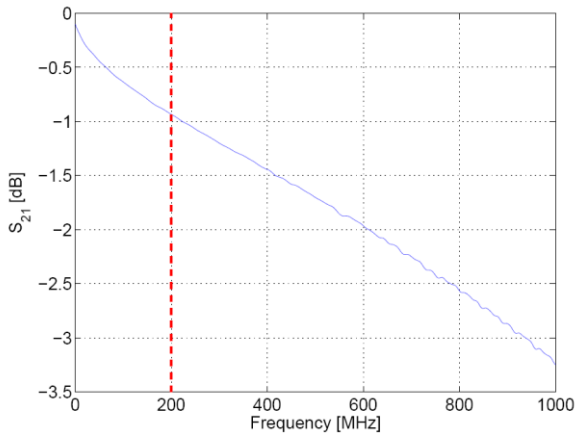

Figure 9: Magnitude of S_{21} over one plate.

The phase response is plotted in Fig. 10 after correction for the meander line electrical length (≈16.7 ns).

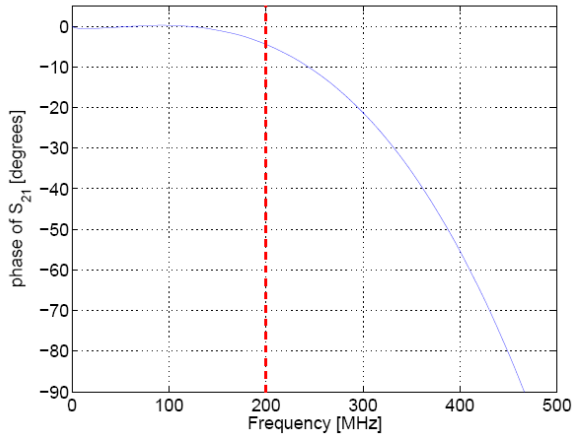

Figure 10: Phase of S_{21} over one plate.

Figure 11 shows a 2 ns rise time input pulse and the corresponding 2.2 ns output pulse. This can be calculated as corresponding to a structure rise time of 1 ns.

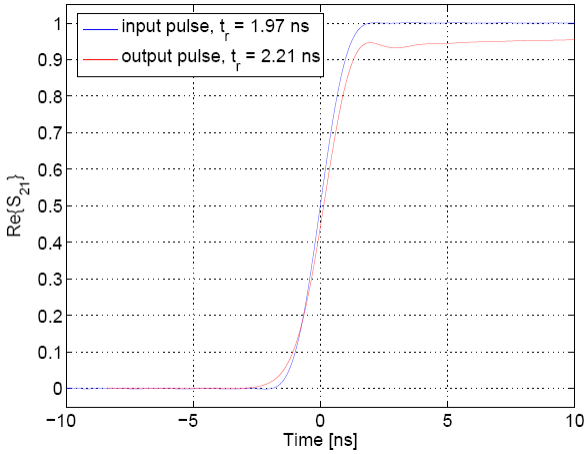

Figure 11: Input and output pulse on the chopper plate.

Input matching has been measured at -26 dB and the structure proved fairly insensitive to the presence of the image plane meaning that the interaction with the other plate will be negligible. Simulations to determine the coverage factor (CF) of the meander line structure were carried out using different tools. A value of CF = 0.78 can be assumed on the beam axis. As an experimental check for the coverage factor simulation, a measurement was performed using a single ceramic plate with a metallic image plane at the beam position (Fig. 12). In the centre of the image plane a 10 mm wide button-type probe measures the electric field at and around the beam position. In order to calibrate the measurement, a reference line consisting of a fully metal-coated plate was used. The measurement confirmed the simulation results.

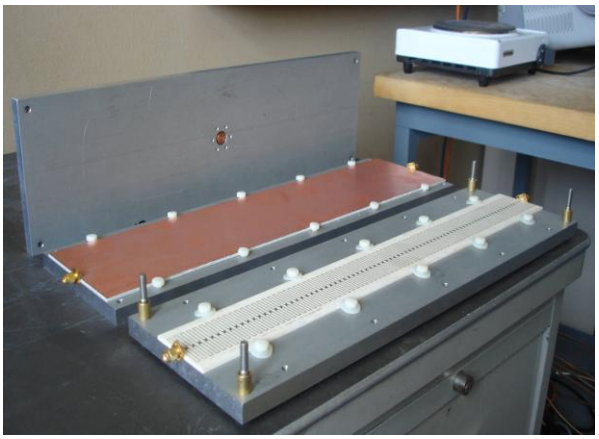

Figure 12: Coverage factor measurement set-up.

3. THE CHOPPER DRIVERS

As far as the chopper driver is concerned, the chopper deflecting structures are essentially two matched 50 Ω transmission lines. They face each other and must be driven with opposite polarity signals with minimum amplitude of 500 V. To avoid perturbations of the accelerated beam, the extraction field must be established or removed within the time separating two bunches (2 ns). For maximum flexibility, the system must be able to remove any number of consecutive bunches (minimum 3) with repetition rates spanning from below 1 MHz to 44 MHz. The required generator is then a high power (5 kW, 5 % duty-cycle), 200 MHz (10 % to 90 %, 2 ns fronts), DC coupled amplifier.

3.1 THE CERN DRIVER

Many active devices and amplification configurations have been considered to achieve the specified requirements that cannot be achieved with a conventional design. A possible solution of the problem was first identified in the idea of generating the low and high frequency parts of the required spectrum with two separate amplifiers[iii]. The two signal are then added at the beam using a tri-axial deflector in which the meander line reference plane is used as a quasi static electrode for the low frequencies. In-depth studies and prototyping have proven the principle but also shown its drawbacks. In fact to sum the two signals correctly they must be perfectly matched in terms of amplitude, phase and timing response. Distortions, saturation effects in the ferrite or in the driving circuits, etc. are then difficult to be kept within the limits required for proper and long term operation. To relax the stringent requirements involved in the unipolar deflecting fields, a second proposal has then been made[iv]. The original single direction beam deflection scheme requires driving one deflector plate positive and the other one negative. The same beam chopping effect can also be obtained by alternating the field polarity as shown in Fig. 13 with the advantage that the DC component self compensates every second cycle. For this reason, this scheme does not need DC coupling and allows the use of wideband transformers for combining large numbers of amplification modules built around RF MOSFETs. Moreover, as the positive and negative pulses are actually generated by separate amplification modules, each path only operates at half the required frequency (i.e. 22 MHz). The extraction of a long sequence of bunches is also possible by simply switching from one polarity to the other as shown in Fig. 14 and adjusting the first and last pulse length.

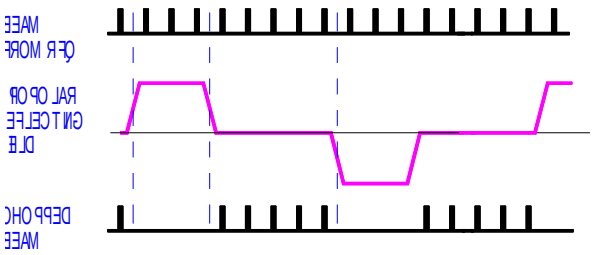

Figure 13: Alternate polarity extraction scheme.

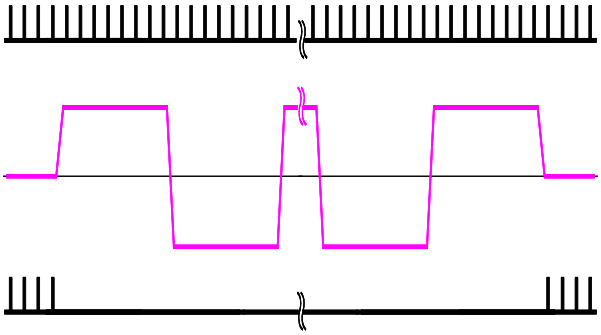

Figure 14: Long extraction sequence.

Based on these considerations a modular system allowing the achievement of the required specifications has been defined and the required components designed, built and tested. Construction has been limited to a half scale prototype (±250 V), and coupling of four such modules would give the required ±500 V. 128 MOSFETs are used to achieve the nominal voltage and individual adjustment of the delay is required in order to minimize the transition fronts.

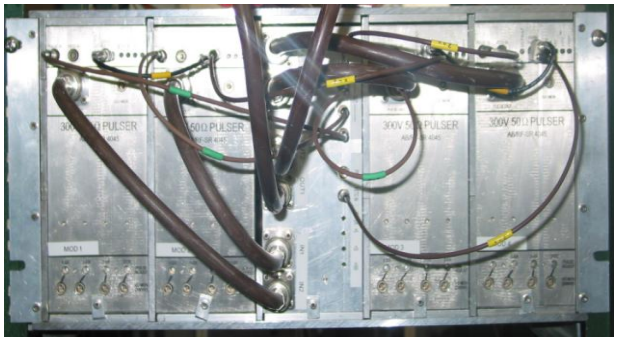

Figure 15: CERN driver ±250 V prototype.

The main characteristics of the prototype are listed in Table 1, Figs. 16 to 18 plot relevant data.

Table 1: 250 V module main characteristics.

Output voltage	± 270 V
Input / Output impedance	50 Ω
Rise / Fall time	≤ 2.1 ns
Repetition frequency	≤ 45 MHz
Burst length	≤ 2 ms
Burst repletion rate	≤ 50 Hz
DC supply	100 V
Cooling	water

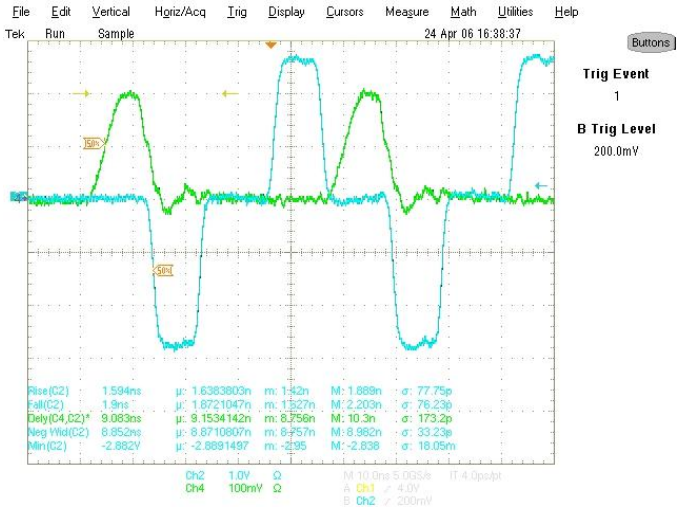

Figure 16: 8.5 ns pulses, 44 MHz chopping
green: input pulse [2 V/div], blue: output pulse [100V/div], abscissa: 10 ns/div

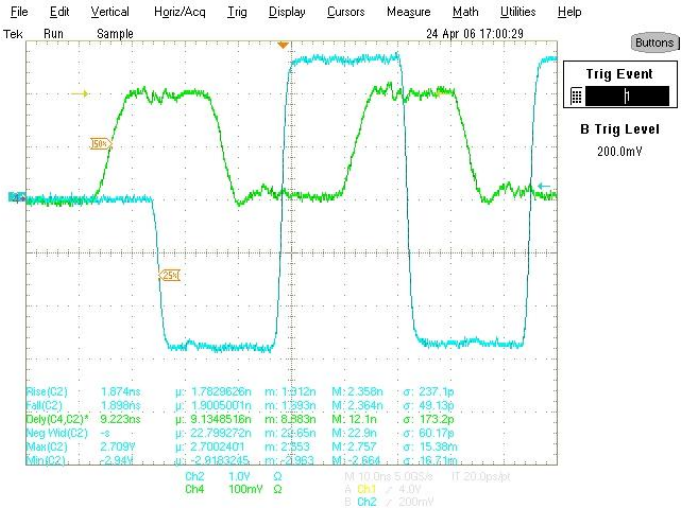

Figure 17: Long bunch sequence chopping.
green: input pulse [2V/div]: blue: output pulse [100V/div], abscissa: 10 ns/div

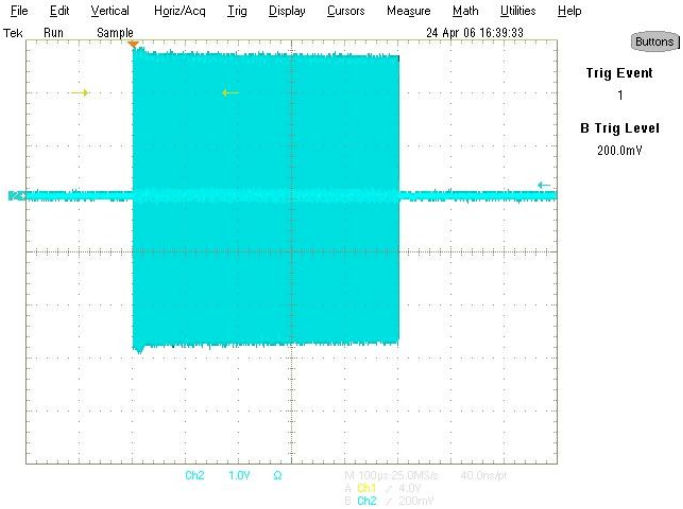

Figure 18: 500 μs burst.
blue: output pulse [100V/div], abscissa: 100 μs/div

The driver delay and pulse length distortion are very important parameters to synchronize the driving signals to the beam. Data plotted in Fig. 19 shows that after the third pulse, the pulse length distortion becomes sufficiently stable and variations are limited to ±100 ps.

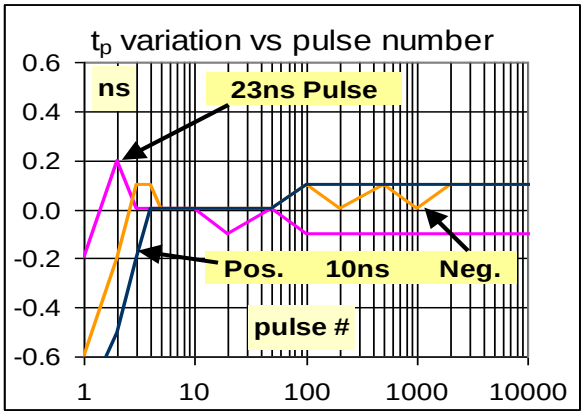

Figure 19: Pulse length distortion within the burst.

The pulse delay plotted in Fig. 20 exhibits variation in the order of ±500 ps (after the 3rd pulse). Moreover, the absolute delay is temperature dependent so that a compensation scheme had to be devised. It is composed of a fast a synchronism detector, an adjustable delay and a digital pulse-to-pulse loop that locks the rising front of the amplifier output pulse to a reference pulse. This compensates slow delay variations (max 30 ps/pulse) over a 10 ns range at working frequency up to 25 MHz. Fig. 21 shows the compensation effect on a test circuit.

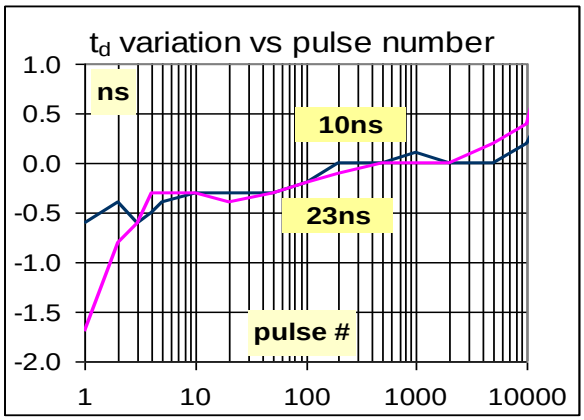

Figure 20: Pulse delay within the burst.

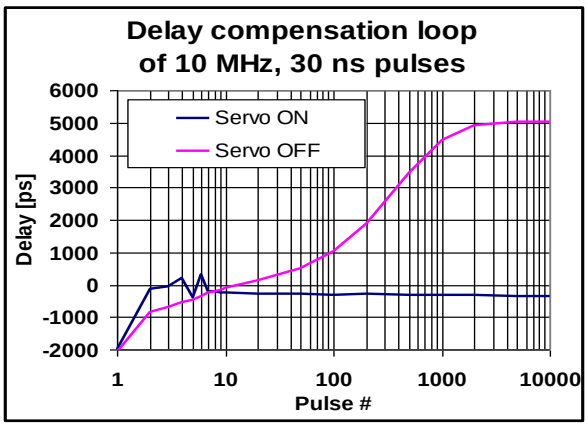

Figure 21: Delay compensation loop.

3.2 THE INDUSTRIAL DRIVER

The CERN driver described above represents a sound solution to the problem of generating the signals for the chopper deflectors. Nevertheless its operation is more complicated when compared to that of a DC coupled amplifier. For this reason, before starting the production of the full set of modules, an additional market survey was carried out with the specification listed in table 2. The only positive answer to the survey came from FID GmbH, the German branch of FID Technology located in St. Petersburg. A visit disclosed a company highly specialized in very fast, high voltage pulse generators based on a proprietary high voltage, high current device (Fast Ionization Dynistor). The main characteristics are superfast switching (<1 ns current rise time), very low resistance and excellent reliability due to uniform current distribution across the device junction. The company's activities include the design and the production of the semiconductor devices as well as their integration into operational pulse generators. The order was placed beginning 2006 for delivery within 12 months but design difficulties and reliability problems delayed the contract completion and presently only one positive output polarity and one negative output polarity prototypes are in house. The present version generators only partially fulfill the specifications as listed in Table 2.

Table 2: Specifications and present status of FID commercial driver.

PARAMETER	REF.	SPEC.	ACHIEVED
Output signal			
Output voltage	V_{out}	700 V	670 V
Load impedance	Z_{out}	50 Ω	OK
Pulse length	T_{Wout}	8 ns to 1 μs	OK
Minimum off pulse time	T_{off}	14 ns	40 ns
T_{off} dep. on T_{Wout}		No	OK
T_{off} dep. on rep. freq.		No	OK
Propagation delay time	T_D	<500 ns	<100 ns
T_D dependent on T_{Wout}		No	No
T_D dep. on rep. freq.		No	Yes
Pulse dist. | T_{Wout} - T_{Win}|	Pd	<5 ns	<3 ns
T_{Pd} dep. on T_{Wout}		No	Yes
T_{Pd} freq.		No	Yes
Maximum rep. freq.	f_{max}	45 MHz	10 MHz
Minimum rep. freq.	f_{min}	Single pulse	OK
Maximum burst length	T_B	1 ms	1 ms
Maximum burst rep. freq.	f_{Bmax}	50 Hz	50 Hz
Rise time (10 % - 90)	T_R	<2 ns	<2.5 ns
Rise time (3 % - 90)	T_{RR}	<2.5 ns	<3 ns
Fall time (90 % - 10)	T_F	<2 ns	<2.5 ns
Fall time (90 % - 3)	T_{FF}	<2.5 ns	<3 ns
Max. voltage between two pulses	$\|V_n\|$	<2 % of V_{out}	<2 %

Figure 22: FID negative pulse generator.

Tests to prove the reliability of the semiconductor devices were made on a preliminary unit that was continuously operated during two weeks producing 1 MHz, 300 ns pulses in 1 ms bursts repeated at 50 Hz. The configuration of the unit was based on a single serial switch that got close to the required transition times but unfortunately could not quite reach the specification. The present version pulse generator (Fig. 22) is built with a different configuration based on a series and a parallel device 1used to start and stop the pulse. These units exhibit a much better rise time, pulse distortion stability and pulse delay stability but with poor reliability. Problems are thought to come from the triggering electronics, which in some situations (i.e. at power turn off) fire simultaneously the two devices that destroy each other. Improved triggering modules are being installed in the positive output unit. Should they prove effective they will be adopted for the whole production.

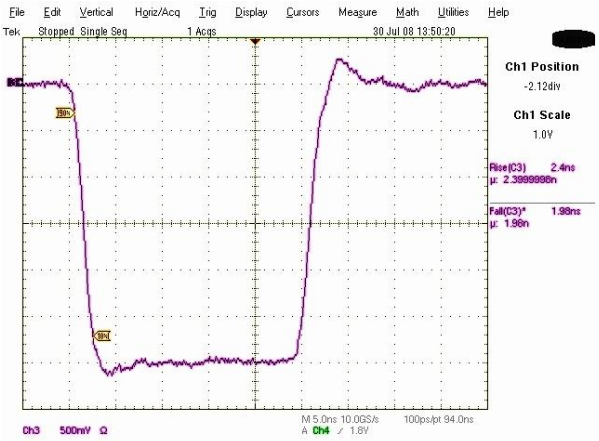

Figure 23: Negative pulse on 50 Ω load,
100V/div, 5 ns/div

The design and production of a new version is being carried out and delivery is expected for the end 2008. Fig.23 shows the output pulse of the negative polarity generator when loaded on a 50 Ω load. Fig. 24 shows the waveforms at the chopper input and output ports. The amplitude attenuation and the effects on the fronts are quite evident as well as the effect of the meander line mismatch that produces reflections. Although significant in the plot, this effect can be easily compensated by a fine adjustment of the load impedance.

Figure 24: Chopper input and output waveforms
Yellow: chopper input, red: chopper output, 100 V/div, 10 ns/div

4 CONCLUSIONS

The fast chopper is an essential part of the CERN Superconducting H- Linac (SPL) and represents a real challenge in all its components. The deflecting structures have been successfully designed, prototyped and tested. They are robust, fairly insensitive to radiation and can stand the required heat load. Two units are ready for installation.
A first pulse generator design based on standard industrial devices has been developed in house. A half scale prototype has been built and fully characterized. It represents a possible solution for driving the chopper deflector and can be readily produced. Nevertheless, a device potentially offering better performance has been ordered from industry. Although still in its prototyping stage and plagued by reliability problems, it is thought to be a more effective solution for this application.

5 ACKNOWLEDGMENTS

We acknowledge the support of the European Community-Research Infrastructure Activity under the FP6 "Structuring the European Research Area" programme (CARE, contract number RII3-CT-2003-506395)

[i] Gerigk, F. (ed), **"Conceptual design of the SPL II: A high-power superconducting H− linac at CERN"**, CERN-2006-006, Geneva (2006)
[ii] T. Kroyer, F. Caspers, E. Mahner, **"The CERN SPL Chopper Structure: A Status Report"**, CERN-AB-2007-004, CARE-Report-06-033-HIPPI
[iii] M. Paoluzzi, **"Design and performance of a 500 V pulse amplifier for the chopper of the CERN superconducting H^- Linac (SPL)"**, CERN/PS 2002-026 (RF), EPAC02
[iv] M. Paoluzzi, **"Status of the CERN chopper driver and the solid state alternative"**, AB-Note-2005-031, CARE/HIPPI Document-2005-003